Complexation of Ni^{2+} and Cu^{2+} by tripodal amine phenol ligands in aqueous solution †

Ashley K. W. Stephens and Chris Orvig*

Department of Chemistry, University of British Columbia, 2036 Main Mall, Vancouver BC, V6T 1Z1, Canada. E-mail: orvig@chem.ubc.ca

The complexation of Ni^{2+} and Cu^{2+} by the tripodal amine phenol ligands 1,2,3-tris(2-hydroxy-5-sulfobenzyl-amino)propane (H$_6$TAPS) and 1,1,1-tris(2-hydroxy-5-sulfobenzylaminomethyl)ethane (H$_6$TAMS) has been studied by potentiometry and UV/VIS spectrophotometry. Both metals form [M(H$_3$L)]$^-$, [M(H$_2$L)]$^{2-}$, [M(HL)]$^{3-}$ and [ML]$^{4-}$ complexes and in addition Cu^{2+} forms [ML(OH)]$^{5-}$ complexes. The complex formation constants for these species have been measured at 25 °C ($I = 0.16$ M NaCl): for Cu^{2+} (Ni^{2+}) with H$_6$TAPS log K{[M(H$_3$L)]$^-$} = 41.73 (36.88), log K{[M(H$_2$L)]$^{2-}$} = 38.53 (31.86), log K{[M(HL)]$^{3-}$} = 34.45 (25.79), log K{[ML]$^{4-}$} = 28.07 (17.53) and log K{[ML(OH)]$^{5-}$} = 18.96. The corresponding values for H$_6$TAMS are 40.20 (36.96), 35.99 (31.91), 29.40 (26.33), 20.20 (18.82) and 9.68. The co-ordination number and geometry of these complexes was investigated by variable pH UV/VIS spectrophotometry; Ni^{2+} and Cu^{2+} show differing complexation behaviour. With both H$_6$TAPS and H$_6$TAMS, Ni^{2+} is co-ordinated by all six ligand donor atoms, probably in an octahedral manner. In the Cu^{2+} complexes the axial sites are only weakly co-ordinating: with H$_6$TAPS the ligand uses an N$_3$O$_2$ donor set to bind Cu^{2+} and the sixth site is occupied by either hydroxide or phenolate oxygen; with H$_6$TAMS, the ligand uses either an N$_2$O$_3$ or an N$_3$O$_2$ donor set to bind Cu^{2+}, and hydroxide co-ordinates in the sixth position.

Introduction

There is considerable interest in the co-ordination chemistry of the lanthanides resulting from their characteristic magnetic properties; for example, the use of Gd–DTPA[1] and Gd–DOTA[2] as MRI agents and various paramagnetic lanthanides used as NMR shift probes [H$_5$DTPA = (carboxy methyl)imino-bis(ethylenenitrilo)tetraacetic acid, H$_4$DOTA = 1,4,7,10-tetra-azacyclododecane-1,4,7,10-tetraacetic acid]. More recently, the magnetic properties of mixed lanthanide–transition metal complexes have been investigated.[3,4] We are currently examining the possibility of aggregating metal ions, with the aim of forming mixed transition metal–lanthanide complexes. Such complexes would be extremely useful for studying the magnetic interactions between metal ions.

The choice of ligand in attempting to prepare such complexes is of paramount importance. The co-ordination and donor atom requirements of both the transition metal ion and the lanthanide must be satisfied. The tripodal amine phenol ligands H$_6$TAPS and H$_6$TAMS contain ideal donor sets for such aggregation: amine nitrogens for the co-ordination of softer transition metals, and phenolate oxygens which will preferentially co-ordinate the harder lanthanides.

Previous research in our group has shown these ligands to be good chelators for Group 13 metal ions[5] and more importantly for lanthanide ions[6] (Ln^{3+}), forming stable complexes with the formulation [Ln(HL)]$^{2-}$ and [LnL]$^{3-}$.[6] More recently, we have been examining the complexation of Ni^{2+}, Cu^{2+} and the lanthanides in the solid state[7] with 1,1,1-tris(2-hydroxybenzyl-aminomethyl)ethane (H$_3$TAM), the non-sulfonated analog of H$_6$TAMS; H$_3$TAM complexes Ni^{2+} and Cu^{2+} to form [Ni-(H$_2$TAM)]PF$_6$ and [Cu(H$_3$TAM)][ClO$_4$]$_2$.[7] We have successfully aggregated transition metals and lanthanides; complexes with the formulation [LnM$_2$(TAM)$_2$]ClO$_4$·xH$_2$O, where M is Ni^{2+} or Cu^{2+}, have been prepared and characterised.[7] We were interested in whether the metal aggregating behaviour exhibited by H$_3$TAM in the solid state (from non-aqueous solvents) could be reproduced in water, where the high solvation energy of the lanthanides would be a greater barrier to the simultaneous complexation of both a trivalent lanthanide and a divalent transition metal ion. We present herein a potentiometric and UV/VIS spectrophotometric study of the complexation of Ni^{2+} and Cu^{2+} with H$_6$TAPS and H$_6$TAMS.

Experimental

Materials

Copper(II), nickel(II) and cobalt(II) atomic absorption standards were purchased from Sigma and Alfa. Water was deionised (Barnstead D8902 and D8904 cartridges) and distilled (Corning MP-1 Megapure still). 1,2,3-tris(2-hydroxy-5-sulfobenzyl-amino)propane (H$_6$TAPS·2.5H$_2$O) and 1,1,1-tris(2-hydroxy-5-sulfobenzylaminomethyl)ethane (H$_6$TAMS·2.5H$_2$O) were prepared as previously described.[5]

Instrumentation

Variable pH UV/VIS spectra were recorded in 10 mm quartz cells on a Shimadzu UV-2100 instrument. The solutions in these cells were held in a thermostated cell holder maintained at 25.0 ± 0.1 °C using a Julabo UC circulating bath.

H$_6$TAPS   H$_6$TAMS

---
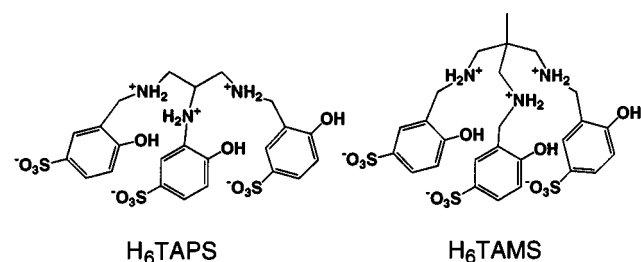
† *Supplementary data available*: variation of ε with pH. For direct electronic access see http://www.rsc.org/suppdata/dt/1998/3049/, otherwise available from BLDSC (No. SUP 57413, 4 pp.) or the RSC Library. See Instructions forAuthors, 1998, Issue 1 (http://www.rsc.org/dalton).

Potentiometric equilibrium measurements

All potentiometric measurements on H_6TAPS and H_6TAMS in the absence, and presence, of metal ions were made with an automatic titrator system consisting of a model 950 Fisher digital pH meter equipped with Orion-Ross glass and calomel reference electrodes, a model 665 Metrohm Dosimat autoburet and water jacketed titration vessels maintained at $25.0 \pm 0.1 °C$ with a Julabo UC circulating bath. Both autoburet and pH meter were interfaced to an IBM compatible personal computer so that the titrations were automated. During the titrations, the solutions were kept under argon that was passed through 2 M NaOH.

The electrodes were calibrated before each titration, and often afterwards, by titrating a known amount of aqueous HCl with a known concentration of NaOH. A plot of mV (calculated) *vs.* pH gave a working slope and intercept so that the pH could be read as $-\log[H^+]$ directly. The value of pK_w used was 13.76.[8]

All solutions were prepared at an ionic strength of 0.16 M NaCl. Carbonate free NaOH ($\approx$0.16 M) was prepared with deionised, distilled water that was boiled and purged with argon while cooling to ensure removal of CO_2. This solution was standardised potentiometrically with potassium hydrogenphthalate. Standard HCl solutions were prepared similarly and were standardised with the NaOH described above. Stock ligand solutions ($\approx$1.0 mM) were prepared using deionised, distilled water and used within 3–4 d. The molecular weight and pK_a of the ligands were always checked whenever a new ligand solution was made and always agreed with previously determined values.[5] The pK_a's for H_6TAPS are; 11.24 (9), 9.77 (6), 8.73 (4), 7.78 (3), 6.54 (2) and 1.7 (1) (where the numbers in parentheses refer to 1σ). The corresponding values for H_6TAMS are 11.19 (4), 9.81 (4), 8.91 (2), 7.95 (3), 6.56 (2) and 2.92 (2). The metal ion solutions were prepared by dilution of the appropriate AA standard. The exact amount of acid present in the AA standards was determined by titration of an equimolar solution of metal standard and Na_2H_2EDTA; the amount of acid in this solution was determined using the Gran method[9] and is equal to the amount of acid in the AA standard plus the 2 equivalents of acid liberated from the complexed $EDTA^{4-}$.

The ratio of ligand to metal used was $1:1 < L:M < 3:1$ and ligand concentrations were between 0.8 and 2.0 mM. A minimum of five titrations was performed for each metal–ligand combination, each about 100 data points over the pH range 2–11. Complexation was usually rapid (1–3 min per point gave a stable pH reading); however, the Ni^{2+}–H_6TAMS system exhibited slow complexation kinetics so 10 to 20 min per data point were allowed. Titration curves at either end of this time range were indistinguishable, indicating sufficient time had been allowed for the system to reach equilibrium.

Variable pH UV/VIS measurements

The variable pH UV/VIS spectra of H_6TAPS, H_6TAMS and their Cu^{2+} and Ni^{2+} complexes (except for Ni^{2+}–H_6TAMS) were recorded by withdrawing aliquots from solutions the pH of which was adjusted by addition of base from the Metrohm Dosimat autoburet used for the potentiometric measurements. The pH was measured in the same way as for the potentiometric measurements. Concentrations were $\approx$0.7 mM for measurements between 360 and 800 nm, 0.3 mM for 300–360 nm and 0.02 mM for <300 nm. Since the complexation of Ni^{2+} by H_6TAMS was slow a batch method was used for this system; a series of 24 solutions (0.16 M NaCl) with a 1:1 L:M ratio was prepared and varying amounts of NaOH were added. These solutions were equilibrated at 25 °C for several days, more than long enough for equilibrium to be reached.

Potentiometric equilibrium calculations

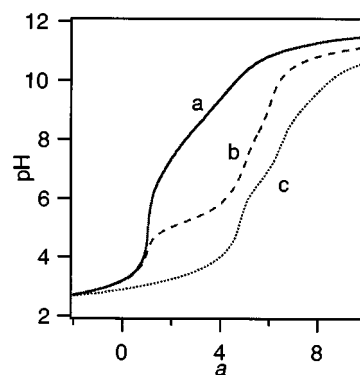The complex stability constants were calculated using the

Fig. 1 Titration curves for (a) H_6TAPS (1.17 mM), (b) Ni^{2+} (0.936 mM) with H_6TAPS (1.03 mM) and (c) Cu^{2+} (0.858 mM) with H_6TAPS (1.03 mM).
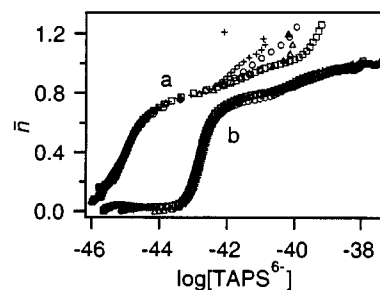

Fig. 2 $\bar{n}$ curves for the (a) Cu^{2+}–H_6TAPS and (b) Ni^{2+}–H_6TAPS systems. The total ligand concentration is $\approx$1 mM; $0.475 < Cu:L < 0.879$ and $0.468 < Ni:L < 0.924$.

program SUPERQUAD.[10] The program sets up simultaneous mass-balance equations for all the components present at each addition of base and calculates the pH at each data point according to the current set of stability constants and the total concentrations of each component. The stability constants are iteratively varied to minimise the sum of the squares of the differences between observed (pH_{obs}) and calculated (pH_{calc}) pH values. The final calculated stability constants are the average of the values determined from individual titrations; an estimate of the error in these values is given by one standard deviation (1σ) for these results.

The calculations allowed for the presence of the hydroxy species $[Ni(OH)]^+$ and $[Cu_2(OH)_2]^{2+}$ for the Ni^{2+} and Cu^{2+} systems, respectively.[11] The final model chosen, which gave the best fit, included the $[M(H_3L)]^-$, $[M(H_2L)]^{2-}$, $[M(HL)]^{3-}$ and $[ML]^{4-}$ species, and with Cu^{2+} the $[ML(OH)]^{5-}$ species. The model was chosen by a combination of trial and error, and from an examination of the titration curves, which gave some indication of the species present, and also the $\bar{n}$ curves,‡ which showed only the presence of mononuclear complexes.[12] Inclusion of other species only worsened the fit, or were rejected during the refinement process.

Results and discussion

Potentiometry

H_6TAPS. Fig. 1 shows the titration curves of Cu^{2+} and Ni^{2+} with H_6TAPS. Complexation of Cu^{2+} occurs below pH 3 [curve (c)] and under more acidic conditions than for Ni^{2+} [curve (b)], which forms the weaker complexes. For Cu^{2+}, various protonated complexes form at pH $\leqslant$ 5, where there is an end-point around $a = 5$ (a = moles of OH^- per moles of ligand), consistent with the ligand binding as $HTAPS^{5-}$. Further complex deprotonations occur, even beyond $a = 6$, which indicate the existence of some hydroxo species. This is also shown by the $\bar{n}$

---

‡ $\bar{n}$ is defined as the average number of ligands (in the most deprotonated form) co-ordinated per metal ion.
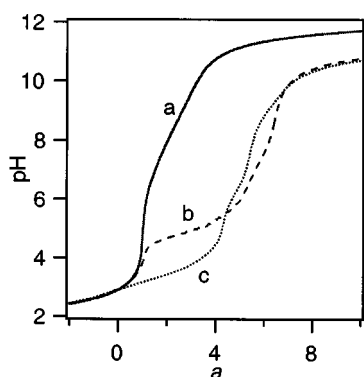
Fig. 3 Titration curves for (a) H_6TAMS (1.426 mM), (b) Ni^{2+} (0.935 mM) with H_6TAMS (1.01 mM) and (c) Cu^{2+} (0.932 mM) with H_6TAPS (1.01 mM).

plot for the Cu^{2+}–H_6TAPS system (Fig. 2); the fractional value of $\bar{n}$ indicates the binding of the ligand in the protonated form. Curves of $\bar{n}$ for different Cu^{2+} concentrations are superimposable only over a limited pH range; at higher pH they diverge and curve back [curve (a)], which is characteristic of the formation of hydroxo complexes.[13] These processes are also accompanied by several colour changes during the titration: as the first protonated complexes form, yellow is observed which rapidly becomes more green as the pH increases, consistent with the binding of increasing numbers of nitrogen donor atoms.[14] No colour changes occur after pH 7, with the most deprotonated complexes being blue-green.

For Ni^{2+} various protonated complexes form until pH 6, where there is an end-point at $a = 5$ [Fig. 1, curve (b)], indicating the ligand is binding as $HTAPS^{5-}$. This is followed by a further deprotonation which is complete by pH 10 ($a = 6$), with the ligand ultimately binding as $TAPS^{6-}$. The $\bar{n}$ curves for Ni^{2+} reflect this [Fig. 2, curve (b)]; various protonated complexes form with $\bar{n}$ having a plateau at 1, indicating the complete formation of $[Ni(TAPS)]^{4-}$. No polynuclear or hydroxo species are indicated, as the $\bar{n}$ curves are superimposable for all Ni^{2+} concentrations.

Titrations with Co^{2+}–H_6TAPS were also performed; however, slow oxidation of the complex occurred. Over the course of the titration a deep brown cobalt(III) complex formed. Saturating the solution with Ar before the titration inhibited the oxidation process, but no reliable measurements of the Co^{2+} complex could be made.

H_6TAMS. Fig. 3 shows titration curves for H_6TAMS with Ni^{2+} and Cu^{2+}. As with H_6TAPS, Cu^{2+} forms the more stable complexes and both metals form protonated species. For Cu^{2+} there is an end-point at about $a = 4$ [pH 5, curve (c)] and another at $a = 5$ (pH 8) indicating that the ligand is binding as H_2TAMS^{4-} and $HTAMS^{5-}$ respectively. Further deprotonation occurs beyond $a = 6$, indicating the formation of some hydroxo complex as observed with the Cu^{2+}–H_6TAPS system. These processes are accompanied by colour changes from yellow, for the most protonated complexes, to green, for the most deprotonated complexes.

For Ni^{2+} similar behaviour to that exhibited with H_6TAPS occurs [Fig. 3, curve (b)], with end-points at $a = 5$ (pH 6.5) and 6 (pH 9.5) consistent with the binding of $HTAPS^{5-}$ and $TAPS^{6-}$, respectively. These observations are supported by the behaviour of the $\bar{n}$ curves (Fig. 4). In the Ni^{2+} system [curve (b)] $\bar{n}$ reaches a plateau at a value of 1, whereas for Cu^{2+} [curve (a)] it reaches a value of ≈ 0.8, and then curves over before $\bar{n} = 1$ is reached, indicating the formation of hydroxo complexes.

Mixed transition metal–lanthanide titrations. Titrations containing $1:1:1$ ratios of Cu^{2+} or Ni^{2+}, La^{3+} and H_6TAPS or H_6TAMS were performed. No evidence for mixed metal
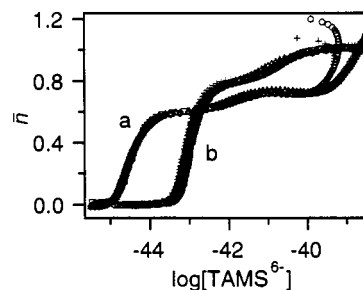

Fig. 4 $\bar{n}$ curves for the (a) Cu^{2+}–H_6TAMS and (b) Ni^{2+}–H_6TAMS systems. The total ligand concentration is ≈ 1 mM; $0.370 < Cu:L < 0.923$ and $0.545 < Ni:L < 0.926$.
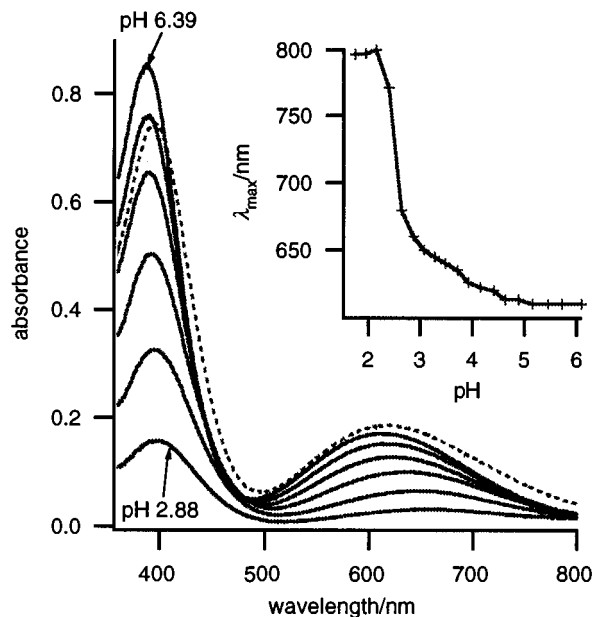

Fig. 5 Visible spectra of $1:1$ 0.707 mM Cu^{2+}–H_6TAPS (solid curve) at pH 2.88, 3.28, 3.71, 4.16, 4.63 and 6.39 and $1:1$ 0.639 mM Cu^{2+}–H_6TAMS (broken curve) at pH 6.13. Inset: variation of λ_{max} with pH for the Cu^{2+}–H_6TAPS system.

complexes was found; in all cases, complexation of the transition metal proceeded as in the absence of lanthanide (*i.e.* as above); lanthanum hydrolysis was observed at pH 7, and lanthanum hydroxide precipitated at pH > 8.

UV/VIS studies

For the Cu^{2+} systems there are two regions of interest in the UV/VIS spectra as shown in Figs. 5 and 6. In the Cu^{2+}–catechol system[15] there is an absorbance maximum at ≈ 410 nm, which was assigned to a ligand–metal charge transfer. Similarly, in the Cu^{2+} L-DOPA [3-(3,4-dihydroxyphenyl)-L-alanine] system a charge transfer band occurs at ≈ 410 nm, indicative of bis(catecholate) type binding.[14,16] No d–d transitions occur at this energy. Thus, the band at ≈ 390 nm in the two Cu^{2+} systems (Fig. 5) is assigned to phenolate–copper charge transfer and changes in absorbance at this wavelength correspond to the extent of phenolate binding. The position of λ_{max} for this band varies only slightly with pH and the strong yellow colour of the protonated complexes arises from this absorption.

The d–d transitions give rise to an absorbance the position of which is diagnostic of the ligand field and co-ordination geometry about Cu^{2+}. In the Cu^{2+}–catechol system λ_{max} for the d–d band of the $[CuL_2]^{2-}$ complex is ≈ 670 nm,[15] whereas in complexes with more amine donor atoms λ_{max} shifts to shorter wavelength, 550 nm for $[Cu(en)_2]^{2+}$ for example.[17] For the Cu^{2+}–H_6TAPS complexes, λ_{max} is between 610 and 670 nm (Fig. 5), depending on pH; for the Cu^{2+}–H_6TAMS complexes, λ_{max} is constant at ≈ 620 nm. These values lie in the range expected
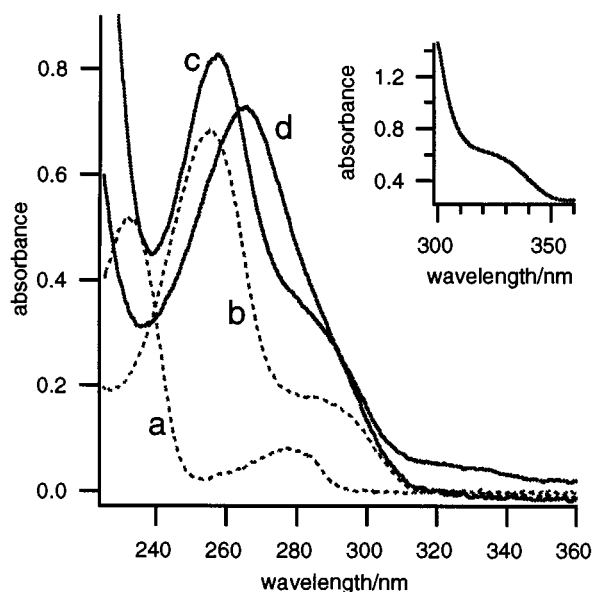
Fig. 6 The UV spectra of (a) 0.0201 mM H_6TAPS, pH 1.95; (b) 0.0201 mM H_6TAPS, pH 11.12; (c) 1 : 1 0.0195 mM Cu^{2+}–H_6TAPS, pH 11.18 and (d) 1 : 1 0.0195 mM Ni^{2+}–H_6TAPS, pH 10.29. Inset: UV spectrum of 1 : 1 0.288 mM Cu^{2+}–H_6TAPS, pH 8.20.

for pseudo-octahedral (octahedral, square planar or square pyramidal) co-ordination geometries. The other possible co-ordination geometry, trigonal bipyramidal, absorbs at much longer wavelength; $[Cu(tren)(NH_3)]^{2+}$ has $\lambda_{max} = 877$ nm for example.[18] The colours of the complexes, ranging from yellow to green, confirm that both oxygen and nitrogen co-ordination exists.

The protonated phenols in H_6TAPS and H_6TAMS have an absorption maximum at ≈230 nm, shifting on deprotonation or complexation to ≈260 nm, and varying somewhat depending on the complex. This is shown for the H_6TAPS systems in Fig. 6; the spectra for the corresponding H_6TAMS systems are almost identical. Changes in absorbance at 260 nm correspond to phenol deprotonation but this is not necessarily synonymous with phenolate co-ordination. In the Cu^{2+} systems there is also a shoulder at ≈325 nm (Fig. 6 inset) which does not seem to be associated with the aromatic moieties; neither of the two ligands, nor their Ni^{2+} complexes, absorbs above 320 nm. This band may be a second ligand–metal charge transfer band and the two different bands may therefore correspond to phenolate oxygens in different environments. As a result of the Jahn–Teller effect and the preference of Cu^{2+} for the amine nitrogens over the phenolate oxygens the three nitrogens will tend to occupy the equatorial positions, if steric effects allow, leaving only one equatorial site plus two axial sites for the phenolate oxygens. Axial and equatorial phenolates will be inequivalent and charge transfer transitions associated with these sites may have different energies and intensities. Alternatively, there may simply be two charge transfer bands for each phenolate, regardless of whether it is co-ordinated axially or equatorially.

The visible spectra of the nickel complexes afford much less information and consequently only the extent of phenolate deprotonation was studied.

## Metal complex stability constants

The stability constants (eqns. 1 and 2) for the Cu^{2+} and Ni^{2+}

$$M^{2+} + L^{6-} + nH^+ \overset{K}{\rightleftharpoons} [M(H_nL)]^{(4-n)-} \quad (1)$$
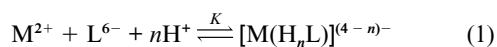
$$K[M(H_nL)^{(4-n)-}] = [M(H_nL)^{(4-n)-}]/[M^{2+}][L^{6-}][H^+]^n \quad (2)$$

complexes of H_6TAPS and H_6TAMS appear in Table 1 and species distribution curves in Fig. 7. Both Cu^{2+} and Ni^{2+} form $[M(H_3L)]^-$, $[M(H_2L)]^{2-}$, $[M(HL)]^{3-}$ and $[ML]^{4-}$ complexes and in addition Cu^{2+} forms $[ML(OH)]^{5-}$. This behaviour is markedly different from that of the Group 13 metals and the lanthanides with these ligands, which form only $[M(HL)]^{2-}$ and $[ML]^{3-}$ species.[5,6] As expected, with both ligands, Cu^{2+} forms more stable complexes than does Ni^{2+}, although the differences are greater for H_6TAPS.

The pK values of the metal complexes (eqns. 3 and 4) also
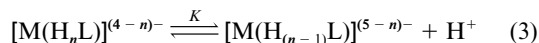
$$[M(H_nL)]^{(4-n)-} \overset{K}{\rightleftharpoons} [M(H_{(n-1)}L)]^{(5-n)-} + H^+ \quad (3)$$

$$K = [MH_{(n-1)}L^{(5-n)-}][H^+]/[MH_nL^{(6-n)-}] \quad (4)$$

appear in Table 1. One trend is apparent; the pK of the complex increases as the charge becomes more negative, consistent with the ease of removing a proton decreasing as the complex becomes more negatively charged. The stabilities of the Cu^{2+} and Ni^{2+} complexes with the hexadentate H_6TAPS and H_6TAMS are significantly higher than those of the tridentate parent amines propane-1,2,3-triamine (TAP) and 1,1,1-tris(aminomethyl)ethane (TAME); log $K([ML]^{2+})$ for Cu^{2+} and Ni^{2+} with TAP§ (TAME¶) = 11.1 (10.97) and 9.3 (10.15), respectively.[19,20]

Although the Cu^{2+}–H_6TAPS and Cu^{2+}-H_6TAMS systems form the same complex species, the stabilities of these species differ markedly. In addition, the pK's of these protonated species also differ significantly, indicating different structures and/or different donor atom sets in each system. The pK_a's (eqns. 5 and 6) for H_6TAPS (H_6TAMS) are 11.24 (11.19), 9.77
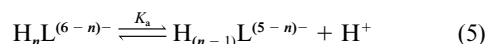
$$H_nL^{(6-n)-} \overset{K_a}{\rightleftharpoons} H_{(n-1)}L^{(5-n)-} + H^+ \quad (5)$$

$$K_a = [H_{(n-1)}L^{(5-n)-}][H^+]/[H_nL^{(6-n)-}] \quad (6)$$

(9.81), 8.73 (8.91), 7.78 (7.95), 6.54 (6.56) and 1.7 (2.92), where the two highest values and the lowest are those of the amine nitrogens and the remaining three are those of the phenolic oxygens.[5] The deprotonation constants of the two ligands are very similar so that differences in stability among the complexes do not arise from this source.

The Ni^{2+}–H_6TAPS and Ni^{2+}-H_6TAMS systems are strikingly similar. Not only are the same species present, but complexes with the same protonation state are of similar stability and more importantly the pK's for these species are also very similar. This suggests that complexes with the same protonation state have similar structures and donor atom sets. More about the order of deprotonation of the ligand donor atoms and the nature of the protonated complexes for both Cu^{2+} and Ni^{2+} can be elucidated with variable pH UV/VIS spectrophotometry, as discussed below.

Metal complex structures

In this section variable pH UV/VIS studies are compared with speciation behaviour in order to probe the solution structures of these complexes in more detail. Speciation curves are concentration dependent; the curves shown in Fig. 7 are valid for the concentrations used to study the d–d and CT bands discussed later, but not for the much lower concentrations used to study the UV region. New speciation curves (not shown) were calculated for these lower concentrations in order to be able to relate the UV and speciation behaviour of these systems.

Cu^{2+}–H_6TAPS. Studies of Cu^{2+} complexes of peptides have established an empirical formula for predicting the λ_{max} of the
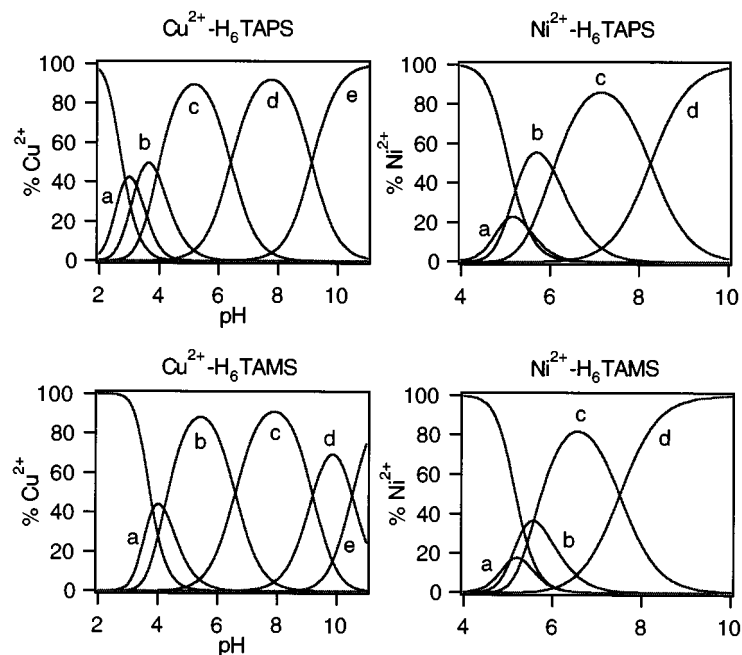
Fig. 7 Speciation diagrams for the M^{2+}–H_6TAPS systems (top) and M^{2+}–H_6TAMS systems (bottom). The species are as follows: (a) $[M(H_3L)]^-$; (b) $[M(H_2L)]^{2-}$; (c) $[M(HL)]^{3-}$; (d) $[ML]^{4-}$; (e) $[ML(OH)]^{5-}$. The total metal and ligand concentrations are 0.7 mM.

Table 1 Stability constants (log K) and deprotonation constants (pK) for Cu^{2+} and Ni^{2+} complexes of H_6TAPS and H_6TAMS (25 °C, $I = 0.16$ M NaCl)

Complex	Cu^{2+}–H_6TAPS	pK	Ni^{2+}–H_6TAPS	pK	Cu^{2+}–H_6TAMS	pK	Ni^{2+}–H_6TAMS	pK
$[M(H_3L)]^-$	41.73(3)	3.20	36.88(3)	5.02	40.20(6)	4.21	36.96(12)	5.05
$[M(H_2L)]^{2-}$	38.53(3)	4.08	31.86(3)	6.07	35.99(5)	6.59	31.91(8)	5.58
$[M(HL)]^{3-}$	34.45(6)	6.38	25.79(4)	8.26	29.40(3)	9.20	26.33(4)	7.51
$[ML]^{4-}$	28.07(9)	9.11	17.53(5)		20.20(4)	10.52	18.82(6)	
$[ML(OH)]^{5-}$	18.96(9)				9.68(5)			

d–d band.[17] The energy of the d–d transition can be expressed as the sum of the individual contributions from the four donor atoms lying in the square plane (equatorial sites) about Cu^{2+} and the contribution from amine nitrogens is considerably higher than that from oxygens. Thus, substitution of nitrogen for oxygen in the equatorial sites will cause a decrease in λ_{max} (axial donor atoms have a minor effect, causing a slight increase in λ_{max}).[17] For the Cu^{2+}–H_6TAPS system, for $2 \leqslant$ pH $\leqslant 5$, λ_{max} systematically decreases from ≈ 800 nm (aqueous Cu^{2+}) at pH 2, to ≈ 610 nm by pH 5 (Fig. 5 inset), after which it remains constant. The substitution of phenolate oxygens for water will also result in a decrease in λ_{max}; for the d–d band of the O_4 $[Cu(CAT)_2]^{2-}$ (CAT = catecholate) complex $\lambda_{max} = 670$ nm.[15] However, H_6TAPS contains only three phenolic oxygens, so that the observed λ_{max} values would suggest at least one N coordinated in all the H_6TAPS complexes and that the ratio of N to O donors (either phenolate oxygen or water) in the equatorial sites increases between pH 2 and 5. From Fig. 7 it may be seen that the $[Cu(H_3TAPS)]^-$, $[Cu(H_2TAPS)]^{2-}$ and $[Cu(HTAPS)]^{3-}$ species are formed successively in this pH range, so that it is likely that in these complexes Cu^{2+} is bound equatorially by one, two and three nitrogens, respectively. Thus, in these three complexes, Cu^{2+} is co-ordinated by NO_3, N_2O_2 and N_3O_2 donor sets, respectively.

Fig. 8 shows the variation in absorption coefficients with pH at 610, 383, 340 and 257 nm for the Cu^{2+} complexes, together with that of the free ligand (255 nm). (For the CT band appearing as a shoulder between 300 and 360 nm at 325 nm and below there was too much overlap with the band at 260 nm for useful analysis so that 340 nm was chosen; the same overlap occurred with the Cu^{2+}–H_6TAMS system.) The curve at 610 nm [Fig. 8, curve (b)] mirrors that of the variation of λ_{max} with pH;
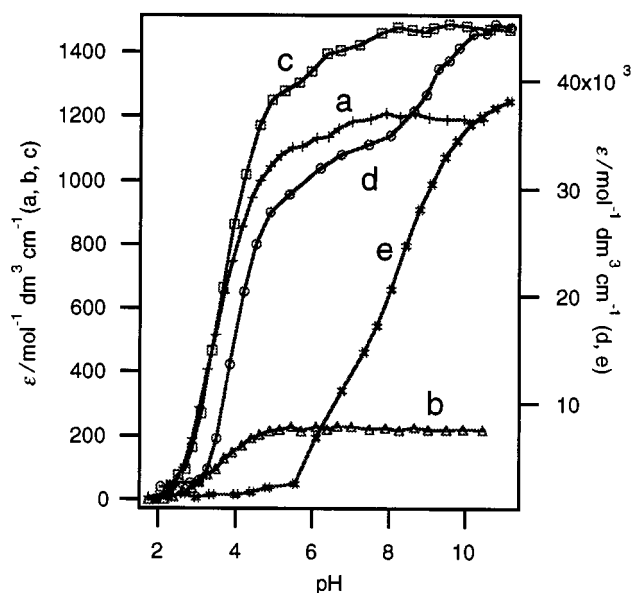

Fig. 8 Variation of ε with pH for 1:1 0.707 mM Cu^{2+}–H_6TAPS at (a) 383; (b) 610 nm; (c) for 1:1 0.288 mM Cu^{2+}–H_6TAPS, 340 nm; (d) for 1:1 0.0195 mM Cu^{2+}–H_6TAPS, 257 nm and (e) for 0.0201 mM H_6TAPS, 255 nm.

above pH 5 the absorbance remains constant, so that the concentration of species containing an N_3O equatorial donor set also remains constant. This agrees well with Fig. 7 which shows that above pH 5 only the $[Cu(HTAPS)]^{3-}$, $[Cu(TAPS)]^{4-}$ and $[Cu(TAPS)(OH)]^{5-}$ species exist and the $[Cu(H_3TAPS)]^-$ and

$[Cu(H_2TAPS)]^{2-}$ species, which have NO_2 and N_2O_2 equatorial donor sets, are negligible. The absorbance profiles of the CT bands at 383 and 340 nm [curves (a) and (c)] are very similar to that of the 610 nm curve. These curves show that phenolate co-ordination is about 90% complete by pH 5. Above pH 5 there is still a slight increase in absorbance until pH 8, suggesting the formation of small amounts of a new complex containing a third co-ordinated phenolate. The variation in ε at 257 nm [Fig. 8, curve (d)], which shows the extent of phenol deprotonation, indicates that by pH 5, approximately 2/3 of total phenol deprotonation has occurred [with the free H_6L, curve (e), phenol deprotonation does not start until pH 6]. These observations agree well with the speciation curves (Fig. 7) which show that at pH 5 the $[Cu(HTAPS)]^{3-}$ species, with two co-ordinated phenolate oxygens, has reached maximum concentration, while those of $[Cu(H_3TAPS)]^-$ and $[Cu(H_2TAPS)]^{2-}$ are negligible. The absorbance at 257 nm increases slightly between pH 5 and 8, more evidence for the existence of a minor complex containing three co-ordinated phenolate oxygens. The curve rises steeply after pH 8 until phenolate deprotonation is complete by pH 10, which must therefore correspond to a complex containing an unco-ordinated phenol group which is being deprotonated. From an examination of Fig. 7 it is apparent that by pH 8 most of the ligand is present as $[Cu(TAPS)]^{4-}$ and $[Cu(TAPS)(OH)]^{5-}$, i.e. completely deprotonated. This implies that the complex $[CuL]^{4-}$ is not simply $[Cu(TAPS)]^{4-}$ but is probably a mixture of $[Cu(HTAPS)(OH)]^{4-}$ and $[Cu(TAPS)]^{4-}$, which are indistinguishable in potentiometric measurements. The inflection point in the 257 nm curve (d) at $\approx$pH 9 should be equal to the pK of the unbound phenol. Inspection of Table 1 shows that the pK of $[Cu(TAPS)]^{4-}$ is 9.11, striking evidence for the existence of $[Cu(HTAPS)(OH)]^{4-}$. As a result of the competition of OH^- for the sixth co-ordination site, the $[Cu(TAPS)]^{4-}$ complex, with three co-ordinated phenolates, is never formed in very high concentrations and the $[Cu(TAPS)(OH)]^{5-}$ complex, with only two co-ordinated phenolates, becomes the dominant species at high pH (Fig. 7).

[Cu(TAPS)]⁴⁻   [Cu(HTAPS)(OH)]⁴⁻   [Cu(TAPS)(OH)]⁵⁻
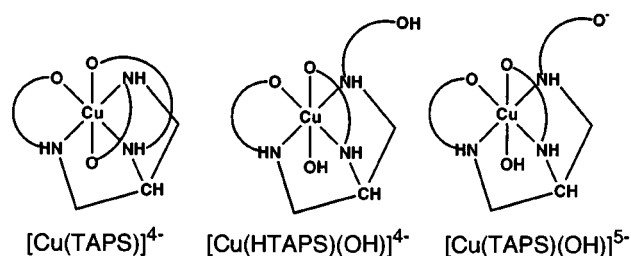
Cu^{2+}–H_6TAMS. The value of λ_{max} for the d–d band of the Cu^{2+} complexes changes very rapidly from that of aqueous Cu^{2+} ($\approx$800 nm) at pH 3.11 to 620 nm at pH 3.50 and is constant thereafter. Using the same arguments presented for the Cu^{2+}–H_6TAPS system, this suggests that from pH 3.5 onwards the number of nitrogen donors in the equatorial sites stays constant. As complexation begins only at pH 3 (Fig. 7), this suggests that all the complexes have the same number of equatorially bonded nitrogens. The only species present until pH 5 are the $[Cu(H_3TAMS)]^-$ and $[Cu(H_2TAMS)]^{2-}$ complexes; λ_{max} = 620 nm suggests that the ligand most likely co-ordinates Cu^{2+} with N_2O and N_2O_2 donor sets, respectively, so that all complexes formed must contain two nitrogens in the equatorial positions.

Fig. 9 shows the variation in ε with pH at 620, 390, 340 and 256 nm, together with the free H_6L curve at 257 nm. The 620 nm curve (b) reaches a plateau by pH 5, in agreement with the speciation curves (Fig. 7), which show that by pH 5 free Cu^{2+} is almost completely complexed. Between pH 3 and 5 the CT bands [curves (c) and (d)] follow the 620 nm curve, showing that the initial complexes contain both co-ordinated N and O. Phenolate co-ordination is mostly complete by pH 5 and 2/3
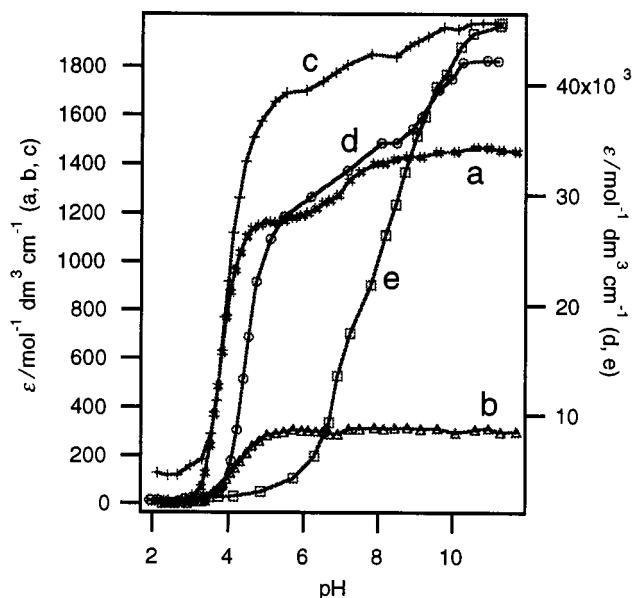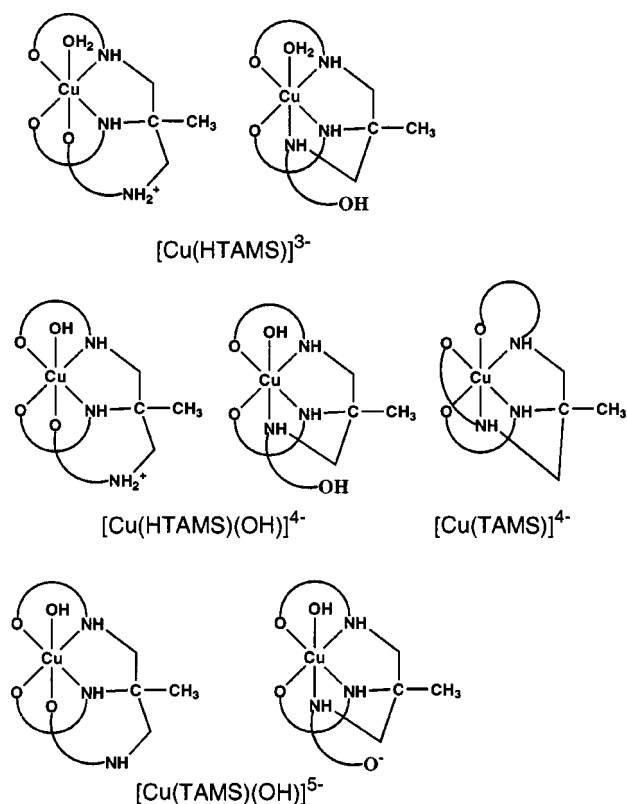

Fig. 9 Variation of ε with pH for 1:1 0.639 mM Cu^{2+}–H_6TAMS at (a) 390; (b) 620 nm; (c) for 1:1 0.312 mM Cu^{2+}–H_6TAMS, 340 nm; (d) for 1:1 0.0187 mM Cu^{2+}–H_6TAMS, 256 nm and (e) for 0.0206 mM H_6TAMS, 257 nm.

total phenolate deprotonation has occurred [curve (a)], consistent with the maximum concentration of $[Cu(H_2TAMS)]^{2-}$ being reached (Fig. 7), and confirming that the complex contains two co-ordinated phenolates in an N_2O_2 donor set. Above pH 5 the system is similar to the Cu^{2+}–H_6TAPS system, except that the species are different. In the Cu^{2+}–H_6TAPS system the $[Cu(HTAPS)]^{3-}$ species is much more stable relative to $[Cu(H_2TAPS)]^{2-}$ than in the Cu^{2+}–H_6TAMS system. This is probably because conversion of $[Cu(H_2L)]^{2-}$ (N_2O_2 donor set) into $[Cu(HL)]^{3-}$ (N_3O_2 donor set) involves co-ordination of N at an equatorial site for H_6TAPS, whereas for H_6TAMS an oxygen co-ordinates.

Between pH 5 and 8 the CT curves and the 256 nm curve are parallel, and the increases in these curves show phenolate deprotonation and co-ordination to form a complex with three co-ordinated phenolates, but this never appears to form completely; after pH 9 the concentration of this species remains constant. However, the absorbance at 256 nm continues to increase until pH 10, showing the existence of a complex with an unco-ordinated phenol group. At pH 5 the $[Cu(H_2TAMS)]^{2-}$ species, with an N_2O_2 donor set, has reached maximum concentration (Fig. 7) so that two co-ordination sites remain to be occupied. After pH 5 the $[Cu(HTAMS)]^{3-}$, $[Cu(TAMS)]^{4-}$ and $[Cu(TAMS)(OH)]^{5-}$ species are successively formed, and all are major species (Fig. 7). Since the $[Cu(TAMS)(OH)]^{5-}$ complex eventually forms to completion at very high pH, one of the co-ordination sites must be occupied by OH^-. Since the complex with three co-ordinated phenolates never forms to completion and there are no complexes with two co-ordinated OH^-, the third amine nitrogen must be competing with the third phenolate oxygen for the final co-ordination site. The pK's of $[Cu(H_2TAMS)]^{2-}$, $[Cu(HTAMS)]^{3-}$ and $[Cu(TAMS)]^{4-}$ are 6.59, 9.20 and 10.52, respectively; these values cannot be assigned to any single process but are associated with the deprotonation of the third nitrogen and oxygen, and that of co-ordinated water to form a hydroxo complex. Thus, after pH 5, a large number of species may exist. The species $[Cu(HTAMS)]^{3-}$ may be a mixture of N_2O_3 and N_3O_2 complexes, $[Cu(TAMS)]^{4-}$ is probably a mixture of N_3O_3 $[Cu(TAMS)]^{4-}$ and $[Cu(HTAMS)(OH)]^{4-}$ (in which $HTAMS^{5-}$ binds Cu^{2+} with either N_3O_2 or N_2O_3 donor sets); in $[Cu(TAMS)(OH)]^{5-}$, the ligand binds Cu^{2+} with either an N_3O_2 or N_2O_3 donor set, and there is an unbound oxygen or nitrogen, respectively.

[Cu(HTAMS)]³⁻ structure (top left)

[Cu(HTAMS)(OH)]⁴⁻ and [Cu(TAMS)]⁴⁻ structures (middle row)

[Cu(TAMS)(OH)]⁵⁻ structure (bottom)

Fig. 10 Variation of ε with pH for (a) 1:1 0.0195 mM Ni^{2+}–H_6TAPS, 265 nm, (b) 0.0201 mM H_6TAPS, 255 nm and (c) % complexation of Ni^{2+} with pH.

Ni^{2+}–H_6TAPS, Ni^{2+}–H_6TAMS. Fig. 10 shows the pH dependence of ε with pH for Ni^{2+}–H_6TAPS at 265 nm, along with that of H_6TAPS (255 nm). Owing to the concentration effect, the speciation curves in Fig. 7 are invalid until pH 7, and the extent of complex formation (calculated at the concentrations used for the UV measurements) has also been plotted. The fact that the absorbance profile [Fig. 10, curve (a)] lags that of the complexation profile [curve (c)] shows that the protonated complexes show mixed N,O co-ordination but contain at least one co-ordinated oxygen. Between pH 7 and 10 the $[Ni(HTAPS)]^{3-}$ complex is deprotonated to the $[Ni(TAPS)]^{4-}$ complex; Fig. 10 shows that phenolate deprotonation continues until pH 10, by which pH formation of $[Ni(TAPS)]^{4-}$ is also complete. This suggests that in $[Ni(HTAPS)]^{3-}$ the ligand uses an N_3O_2 donor set to co-ordinate Ni^{2+} and, upon conversion into $[Ni(TAPS)]^{4-}$, a phenol oxygen deprotonates and binds Ni^{2+}. The crystal structures of the Al^{3+} and Ga^{3+} complexes with non-sulfonated analogues of H_6TAMS and H_6TAPS show both metal ions co-ordinated by N_3O_3 donor sets in slightly distorted octahedral environments.[21,22] The ionic radius of six-co-ordinate Ni^{2+} (0.690 Å) lies close to those of Al^{3+} (0.535 Å) and Ga^{3+} (0.620 Å),[23] so that pseudo octahedral co-ordination of Ni^{2+} by H_6TAPS is sterically possible.

The UV absorbance profile for the Ni^{2+}–H_6TAMS system (SUP 57413) is very similar to that for the H_6TAPS case. The Ni^{2+}–H_6TAMS curve (267 nm) rises less steeply than that of the complexation curve, indicative of mixed N,O initial co-ordination, although the two curves lie quite close to each other, suggesting that the complexes formed initially $\{[Ni(H_3TAPS)]^-, [Ni(H_2TAPS)]^{2-}$ and $[Ni(HTAPS)]^{3-}\}$ may all contain two co-ordinated phenolates. Phenolate deprotonation continues over the range pH 4–10, which shows that the formation of $[Ni(TAMS)]^{4-}$ involves the deprotonation and co-ordination of the third phenolic oxygen, as occurred with H_6TAPS. Octahedral co-ordination of Ni^{2+} by $TAMS^{4-}$ is expected, although as with $[Ni(TAPS)]^{4-}$ the exact donor atom arrangement cannot be determined.

The much lower stability of the H_6TAMS complexes of Cu^{2+}, compared with those of H_6TAPS, is intriguing, especially considering the similarity between the two Ni^{2+} complex
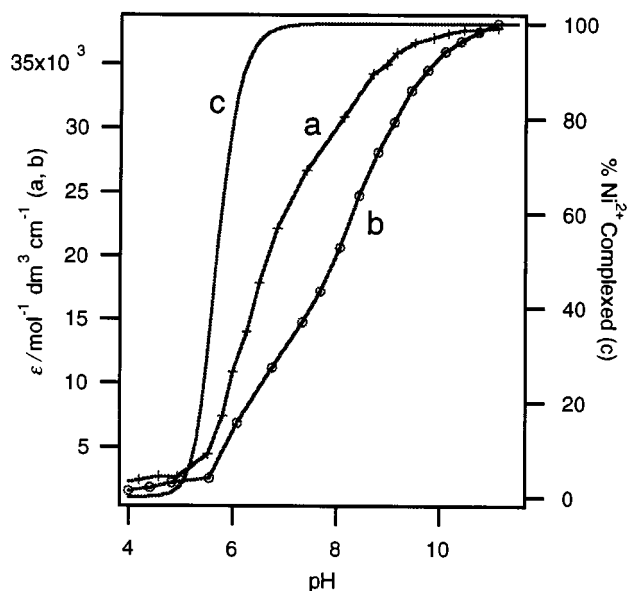
systems. In both Ni^{2+} complexes the ligand can readily co-ordinate Ni^{2+} in a hexadentate fashion, and the structures and stabilities of the complexes are very similar. From the UV/VIS studies above we have detected some structural differences between the Cu^{2+} complexes of the two ligands. In pseudo-octahedral Cu^{2+} complexes the most stable arrangement will favour the maximum number of nitrogens co-ordinated in the square plane about Cu^{2+}. We have shown that this is the case for the $[M(HL)]^{3-}$, $[ML]^{4-}$ and $[ML(OH)]^{5-}$ complexes of H_6TAPS, whereas only two nitrogens bind equatorially in the corresponding H_6TAMS complexes, which are much less stable, and the third nitrogen binds weakly in an axial position. This must be due to steric reasons, although it is not immediately apparent why this is so. The differences in stability are much less for the $[M(H_3L)]^-$ and $[M(H_2L)]^{2-}$ complexes. This supports the argument that in these complexes H_6TAPS binds Cu^{2+} with only one and two nitrogens, respectively, whereas H_6TAMS binds Cu^{2+} with two nitrogens in all of its complexes.

Mixed transition metal–lanthanide complexes and metal aggregation

Table 2 shows the stability constants of some of the Cu^{2+} and Ni^{2+} complexes of H_6TAPS and H_6TAMS, together with those of selected lanthanides.[6] The stability constants for the lanthanide complexes are considerably lower than those of their Cu^{2+} and Ni^{2+} analogues and the tendency to form protonated complexes is much lower, with $[Ln(HL)]^{2-}$ the only protonated species found.[6] The ideal scenario for mixed metal complexation would be to have the transition metal co-ordinated by the nitrogen donor atoms and the harder lanthanides binding the phenolate oxygens, as observed in the solid state.[7] We have demonstrated, however, that in water all the metal complexes of Cu^{2+} and Ni^{2+} contain mixed N,O co-ordination. Thus, given the structure and high stability of the transition metal complexes of H_6TAPS and H_6TAMS, it is perhaps not surprising that the additional binding of lanthanides is not thermodynamically favoured in aqueous solution.

Conclusion

Although these studies show that these ligands do not aggregate transition and lanthanide metal ions in water, we have demonstrated that H_6TAPS and H_6TAMS show interesting solution chemistry in their complexation of Ni^{2+} and Cu^{2+}, with a wide

Table 2 Stability constants (log K) for selected complexes of H_6TAPS and H_6TAMS (25 °C, I = 0.16 M NaCl)

Complex[a]	Cu^{2+}	Ni^{2+}	La^{3+}[b]	Nd^{3+}[b]	Gd^{3+}[b]	Ho^{3+}[b]	Yb^{3+}[b]
[M(HTAPS)]	34.45	25.79	18.47	20.13	20.88	21.15	21.54
[M(TAPS)]	28.07	17.53	11.33	13.59	14.50	14.71	15.15
[M(HTAMS)]	29.40	26.33			18.41	19.4	20.11
[M(TAMS)]	20.20	18.82	9.17	11.19	11.86	12.71	13.78

[a] The charges are omitted for simplicity. [b] Ref. 6.

range of complexes being formed. In addition, we have shown that variable pH UV/VIS spectrophotometry is a powerful tool when used in conjunction with pH potentiometry to study these systems; we have been able to determine complex structure and demonstrate the existence of complexes that are indistinguishable by potentiometry alone. The minor change in the amine backbone in going from H_6TAPS to H_6TAMS has a negligible effect in Ni^{2+} complexation but a profound effect in that of Cu^{2+}. The preference of Cu^{2+} for having the maximum number of nitrogen donor atoms in the square plane containing Cu^{2+} apparently cannot be met by H_6TAMS, and the resulting decrease in the stability of its Cu^{2+} complexes compared with those of H_6TAPS is rather profound.

As far as aggregating metal ions in solution is concerned, the absence of mixed transition metal–lanthanide complexes in water in this study should not be considered too discouraging. The formation of the $[LnM_2(TAM)_2]ClO_4 \cdot xH_2O$ complexes in the solid state[7] demonstrates that this type of ligand is indeed the correct choice for metal aggregation from non-aqueous solvents. The co-ordination requirements of the lanthanide are met by the binding of two ligands and additional solvent molecules; in water, however, such complexes are disfavoured. A ligand containing additional amine nitrogens and phenolate oxygens, so that a single ligand can simultaneously satisfy the requirements of both transition metal and lanthanide, may be the next generation of tripodal amine phenol ligands.

References

1 A. D. Watson, *J. Alloys Compd.*, 1994, **207/208**, 14.
2 K. Kumar, T. Jin, X. Wang, J. F. Desreux and M. F. Tweedle, *Inorg. Chem.*, 1994, **33**, 3823.
3 O. Kahn, *Struct. Bonding* (*Berlin*), 1987, **68**, 89; *Adv. Inorg. Chem.*, 1995, **43**, 179; *Molecular Magnetism*, VCH, New York, 1993.
4 E. K. Brechin, S. G. Harris, S. Parsons and R. E. P. Winpenny, *J. Chem. Soc., Dalton Trans.*, 1997, 1665.
5 P. Caravan and C. Orvig, *Inorg. Chem.*, 1997, **36**, 236.
6 P. Caravan, M. P. Lowe, S. J. Rettig and C. Orvig, *Inorg. Chem.*, 1998, **37**, 1637.
7 P. W. Read and C. Orvig, unpublished work.
8 A. E. Martell and R. J. Motekaitis, *Determination and Use of Stability Constants*, VCH, New York, 1988, p. 4.
9 G. Gran, *Acta Chem. Scand.*, 1950, **4**, 559.
10 P. Gans, A. Sabatini and A. Vacca, *J. Chem. Soc., Dalton Trans.*, 1985, 1195.
11 C. F. Baes, jun. and R. E. Mesmer, *The Hydrolysis of Cations*, Wiley, New York, 2nd edn., 1976.
12 F. J. Rossotti and H. Rossotti, *The Determination of Stability Constants and Other Equilibrium Constants in Solution*, McGraw-Hill, New York, 1961.
13 T. G. Lutz, D. J. Clevette, H. R. Hoveyda, V. Karunaratne, A. Nordin, S. Sjöberg, M. Winter and C. Orvig, *Can. J. Chem.*, 1994, **72**, 1362.
14 A. Gergely and T. Kiss, *Inorg. Chim. Acta*, 1976, **16**, 51.
15 F. Röhrscheid, A. L. Balch and R. H. Holm, *Inorg. Chem.*, 1966, **5**, 1542.
16 W.-L. Kwik, E. Purdy and E. I. Stiefel, *J. Am. Chem. Soc.*, 1974, **96**, 1638.
17 E. J. Billo, *Inorg. Nucl. Chem. Lett.*, 1974, **10**, 613.
18 M. Duggan, N. Ray, B. Hathaway, G. Tomlinson, P. Brint and K. Pelin, *J. Chem. Soc., Dalton Trans.*, 1980, 1342.
19 J. Prue and G. Schwarzenbach, *Helv. Chim. Acta*, 1950, **33**, 995.
20 A. Sabatini and A. Vacca, *J. Chem. Soc., Dalton Trans.*, 1980, 519.
21 S. Liu, E. Wong, V. Karunaratne, S. J. Rettig and C. Orvig, *Inorg. Chem.*, 1993, **32**, 1756.
22 S. Liu, E. Wong, S. J. Retting and C. Orvig, *Inorg. Chem.*, 1993, **32**, 4268.
23 R. D. Shannon, *Acta Crystallogr., Sect A*, 1976, **32**, 751.

Paper 8/03113D